



An Investigation into the Deep Drawing of Fiber-metal Laminates based on Glass Fiber Reinforced Polypropylene

A. Rajabi, M. Kadkhodayan*

Department of Mechanical Engineering, Ferdowsi University of Mashhad, Mashhad

PAPER INFO

Paper history:

Received 27 June 2013

Received in revised form 28 August 2013

Accepted 14 September 2013

Keywords:

Deep Drawing

Fiber-metal Laminate

Design of Experiments

Finite Element Analysis

ABSTRACT

Fiber-metal laminates (FMLs) are new type of composite materials which could improve defects of traditional composites in ductility, formability, impact and damage tolerance. Drawing behavior of a thermoplastic based FML consisting of glass-fiber reinforced polypropylene laminate as the core and aluminum AA1200-O as skin layers was investigated. The effects of process variables consisting of blank-holder force, temperature, blank diameter and blank thickness on the forming behavior of the FML were studied. To reduce the number of experiments and investigate process variables on maximum drawing force and wrinkling of specimens, design of experiments was used. The experimental results were indicated that the general effects of blank-holder force on the failure mode in FMLs and the effects of blank diameter and blank thickness of a FML in deep drawing was similar to custom metals. Furthermore, results demonstrated that a high interaction between temperature and blank-holder force was required to remove the wrinkling. Engineering constants of GFRP were obtained using Timoshenko's beam theory. Numerical simulations were performed by the finite element software, ABAQUS, and a good agreement was observed between the numerical and experimental data.

doi: 10.5829/idosi.ije.2014.27.03c.01

1. INTRODUCTION

Deep drawing is one of the most important sheet forming processes which is used in the automotive, home appliance and aerospace fields. The limits of this process are the onset of wrinkling, fracture failure and drawn-in failure. In order to meet great market demands for lighter, safer and cheaper formed products, it is necessary to select the proper drawing parameters which influence the drawing operation [1]. The latest researches on the deep drawing process and its effective parameters include the following: Padmanabhan, et al. [2] studied the significance of three important process variables namely, die radius, blank holder force and friction coefficient on the deep drawing characteristics of a stainless steel axi-symmetric cup. An investigation on the limit drawing ratio, punch force and minimum wall thickness based on the parameter full factorial experimentation in the optimization of deep drawing process was performed by Özek and Ünal [3]. Arab and

Nazaryan [4] studied the deep drawing of circular blanks in axi-symmetric cylindrical cups forming using numerical modeling. They introduced an analysis tool for the design of any cup drawing process. Rezaiee-Pajand and Moayyedean [5] investigated two-dimensional plane stress wrinkling model of a plastic annular plate. They used energy method and nonlinear strain-displacement law.

In deep drawing process wrinkling can occur in critical regions of the blank subjected to compressive stresses. The conditions for the onset of wrinkling are controlled by the local geometry (sheet curvature) and the current state of stress. Correia and Ferron [6] studied the onset of wrinkling in anisotropic metal sheets under deep drawing by using an analytical approach and finite element simulations. Previous investigation on the channel forming of thermoplastic FML systems by Mosse et al. [7] illustrated the effect of preheating the laminate. It was shown that an increase in preheat temperature improves springback and reduces failure in the FML. The studies carried out by Mosse et al. [8] demonstrated effects of preheat temperature and core material properties on the rectangular cup forming of

*Corresponding Author Email: kadkhoda@um.ac.ir (M. Kadkhodayan)

FML. A glass-fiber reinforced polypropylene core based FML (GFRP based FML) showed lots of wrinkles in the flange, while the self-reinforced polypropylene composite core (SRPP) exhibited significant splitting of the aluminum skin layers with no indication of wrinkling. Research on the drawing behavior of metal-composite sandwich structures by Gresham et al. [9] showed the effect of constituent material properties and the process variables of blank preheat temperature and blank-holder force on the formability of FML systems. Experiments showed that the blank-holder force has a primary effect on the failure mode of FML, i.e. lower forces resulting in wrinkling and higher forces resulting in tearing and fracture.

In the last decades the finite element method (FEM) has been used for the deep drawing analysis of multi-layers metal sheets. However, few numerical researches have been reported on the deep drawing analysis of composite laminates and fiber metal laminates. Morovati et al. [10] studied the wrinkling of two-layer (aluminum-stainless steel) sheets in the deep drawing process through an analytical method, numerical simulation and experiments. The effects of several parameters on the deep drawing process of laminated metal sheets were studied by Atrian and Fereshteh-Saniee [11]. Their main aim was taking the advantages of different materials, such as high strength, low density and corrosion resistibility at the same time and in a single blank. Davey et al. [12] developed a finite element model to simulate the stamp forming of CF/PEEK sheets. This model was validated based on stamp forming experiments performed under various blank holder forces in which the evolution of strain was measured and compared to the results of finite element simulations.

In the current study, a thermo-plastic based FML which is a new type of composite materials was manufactured and its deep drawing process was investigated experimentally and numerically. The main objective of the present study is to study the effect of blank-holder force, temperature and blank geometry on the formability of the new laminate in deep drawing process.

2. MATERIAL

2.1. Laminate Preparation A type of thermoplastic fiber-metal laminates with two thicknesses and two diameter discs was manufactured based on glass-fiber reinforced polypropylene laminate (GFRP) and aluminum AA1200-O as the core and skin layers, respectively. The thickness of aluminum was 0.5 mm and composite laminates had two thicknesses of 1 and 2 mm. A hot plate press was used to manufacture the glass-fiber reinforced polypropylene panel, polypropylene film

stacking and fiber impregnation (Figure 1-a). The composite core was sandwiched between two layers of cleaned aluminum sheet by applying a 0.2 mm thick layer of a hot-melt polypropylene adhesive (PP-g-MAH) that was placed at each bi-material interface, as shown in Figure 1-b. The laminate was consolidated by heating to 200°C in the hot plate press for 10 min and the total thickness of FMLs was 2 and 3 mm. Before performing the deep drawing operation, the laminates were trimmed to 110 and 120 mm diameter discs by removing burrs from the edge of the discs. Figure 2 shows a prepared laminate blank.

2.2. Mechanical Properties According to ASTM E8 M-04 and ASTM D 3039-0, at least three tensile specimens were fabricated for each of the materials, aluminum, fiber reinforced polymer composite and FML. Tensile tests were conducted at constant strain rate of 0.2 min⁻¹ and 0.01 min⁻¹ for aluminum 1200-O and laminates, respectively, using Zwick Z250 machine as explained in ASTM Standards [13]. The stress-strain curves of FML and its constituents are shown in Figure 3. Table 1 shows the mechanical properties of these materials. The average values and standard deviations of σ_{ut} are reported in the table, while the elastic moduli of the materials were the same. The total elongations were not measured for the specimens.

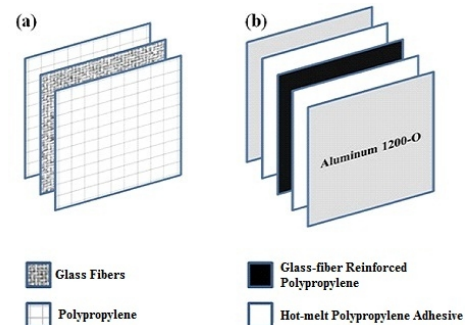


Figure 1. (a) Schematic illustration of composite layup, (b) Schematic illustration of FML layup.



Figure 2. Image of the fiber-metal laminate specimen preparation.

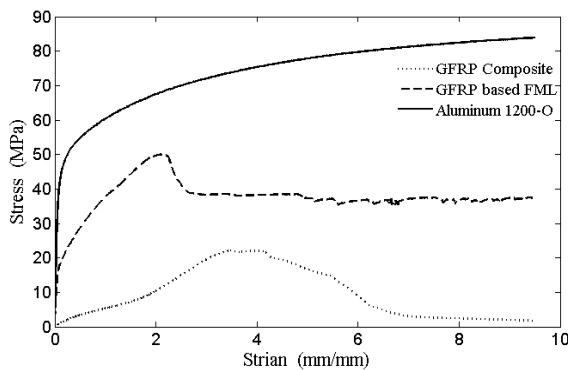


Figure 3. Stress-strain curve for materials used in experiments.

Full annealed aluminum sheet showed isotropic behavior during tensile test, hence it is assumed that aluminum sheet had no anisotropy during simulation. Moreover, the GFRP is a woven composite and was modeled as a composite material. Thus, to consider the proper anisotropy its material constants should be found. Engineering constants of the GFRP lamina consisting of E_{11} , E_{22} , G_{12} , G_{13} , G_{23} and ν_{12} are shown in Table 2. As mentioned, the GFRP is a polypropylene based composite with woven glass fiber; therefore, E_{11} , G_{13} and ν_{12} will be equal to E_{22} , G_{23} and ν_{21} respectively. The three-point bending test is a flexural test to determine the shear modulus. The test method for a rectangular cross section isotropic beam based on well-known Timoshenko beam theory [14] is given by the following equation:

$$w = \frac{PL^3}{4Eb^3} + \frac{PL}{4K_sGb} \quad (1)$$

TABLE 1. Material properties used in experiments

Quantity	Aluminum 1200-O	Glass-fiber reinforced polypropylene	GFRP based FML
Ultimate tensile stress σ_{ut} (MPa)	89.3 ± 0.9	22.6 ± 0.6	47 ± 3
Longitudinal elastic modulus E_{11} (GPa)	68.5	0.94	30
Elongation %	30	14	30

TABLE 2. Measured material constants for using in finite element analysis

Material	E_{11} (GPa)	E_{22} (GPa)	G_{12} (GPa)	G_{13} (GPa)	G_{23} (GPa)	ν_{12}
Glass-fiber reinforced polypropylene	0.94	0.94	0.083	0.034	0.034	0.36

where W is deflection of the beam, P applied load, L span, b width, h thickness, and E and G are elastic and shear module, respectively. The parameter k_s is the so-called “shear correction factor” and $\approx \frac{5}{6} = 0.833$ [15].

Kennedy, et al. [16] and Timoshenko [17] stated that, Equation (1) can be used for orthotropic beams; in fact, there is no relation between shear and normal stresses

In order to use this equation for orthotropic beams when the longitudinal axis of the beam coincides with the fiber direction, E equals E_{11} , and G coincides with G_{13} , provided the thickness of the lamina is perpendicular to the beam width. Equation (1) is obtained with the assumption that the length of the beam is large enough compared to its width. In case this condition does not occur or in order to obtain more accuracy, the general stiffness matrix of orthotropic materials can be used and, E_{11} must be replaced with $E_{11}/(1-\nu_{12}\nu_{21})$ [14].

When both sides of Equation (1) is divided by $PL^3/4bh^3$, it is convenient to rewrite this equation in the following form:

$$\frac{1}{E_f} = \frac{1}{E_{11}} + \frac{1}{K_s G_{13}} \left(\frac{h}{L} \right)^2 \quad (2)$$

where

$$E_f = \frac{E^3}{48I} \left(\frac{P}{w} \right) \quad (3)$$

In Equation (2), E_f is the apparent modulus of elasticity (GPa), L the span (mm), I the second moment of area (mm^4) and P/w the slope of the load-deflection curve (N/mm).

In order to determine the shear modulus and true modulus of elasticity, according to the ASTM D790-03, several three-point bending tests with different h and L of beams were performed on the GFRP samples at a strain rate of 0.01 min^{-1} . Plotting $1/E_f$ against $(h/L)^2$ and doing a linear regression of data would result in a first-degree polynomial. Then, the slope and intercept with the y-axis would provide the shear and true modulus of elasticity, respectively (Figure 4).

Putting $k_s = 0.833$ in Equation (2), the solid line in the figure gave $E_{11} = 1.08$ GPa and $G_{13} = 0.034$ GPa. To obtain Poisson's ratio ν_{12} , the longitudinal modulus E_{11} is replaced with the quantity $E_{11}/(1-\nu_{12}\nu_{21})$ in Equation (2) and E_{11} in the numerator of this fraction is substituted with longitudinal modulus in Table 1, $E_{11} = 0.94$ GPa obtained from tensile test. Solving the relation $0.94/(1-\nu_{12}\nu_{21}) = 1.08$ would result $\nu_{12} = 0.36$. The G_{12} was determined by using the well-known rule of mixtures, $G_{12} = 0.083$ GPa.

3. FINITE ELEMENT ANALYSIS OF DEEP DRAWING

To investigate the deep drawing process of fiber-metal laminates numerically, the ABAQUS 6.9 was used. Because of the wrinkling, the problem is not axisymmetric and a 3D model was applied which increased the computation time. The explicit shell element SC8R with settings (8-node quadrilateral in-plane general-purpose continuum shell, reduced integration with hourglass control, finite membrane strains) was used. The thickness of the plate was divided into three parts. The upper and lower parts were aluminum and the middle part was composite. The required material properties for the analysis were obtained from the stress-strain curve in Figure 3 and the material constants in Table 2. In addition, densities were inserted into the software due to the Dynamic-Explicit analysis. For the details of Dynamic-Explicit analysis see ABAQUS Manual [18] and references cited therein. To reduce the computation time, the die, punch and blank-holder were assumed to be rigid. The dimensions of die parts are shown in Table 3. Figure 5 shows the finite element model for the analysis of the deep drawing process. The boundary conditions of the model are according to the experimental set up explained in next section. To treat the contact between the different parts, it was assumed that the contact property between the blank and die parts obeyed the coulomb's law, and the friction coefficients of 0.23, 0.2 and 0.18 were applied for contact between plate with punch, blank-holder and die, respectively.

The coefficients of friction were measured experimentally between each part of set up and aluminum as shown in Figure 6. The effect of delamination was ignored in the modeling [19].

4. EXPERIMENTAL PROCEDURE

4. 1. Experimental Setup Deep drawing of laminates was achieved using a 60 ton hydraulic press and a die set with blank-holder as shown in Figure 7. To measure the force of the forming process and the displacement of punch, pressure transmitter and linear magnetic displacement sensor were installed on the press. The die and cylindrical punch with 70 mm and 64.5 mm diameters, respectively, were made of SPK steel and the blank-holder was made of MO40 steel. Other parts of the die set were made of CK45 steel. The

force of blank-holder was provided by using eight B/32/051 springs with the same free length of 51 mm and $K=134$ N/mm were installed around the blank-holder. No lubrication was used during the experiments.

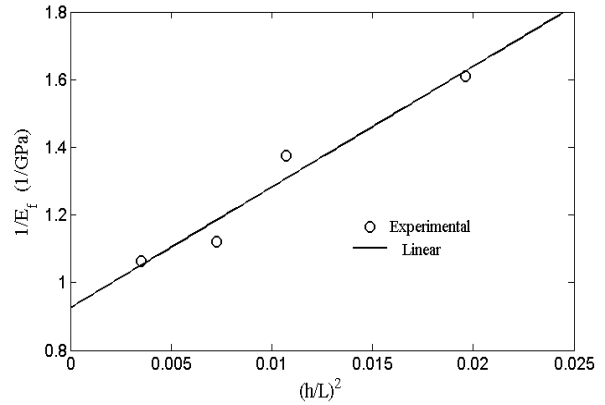


Figure 4. Graphical solution for shear modulus and true modulus of elasticity.

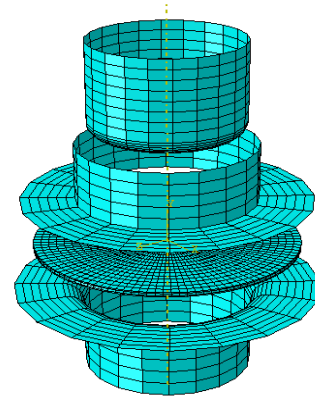


Figure 5. The schematic of the model for FE analysis.



Figure 6. Measurement of friction coefficients

TABLE 3. Dimensions of die parts

	Die diameter	Punch diameter	Outer diameter of blank-holder	Inner diameter of blank-holder	Fillet of die	Fillet of punch
Amount (mm)	70	64.5	160	75	9	6

4. 2. Design of Experiment Design of Experiments was used to reduce the number of experiments and to investigate the process variables on wrinkling of the specimens. The factors of blank-holder force, temperature, blank diameter and blank thickness were identified as important variables that may influence the forming behavior of a FML. The levels for the factors were:

- (1) Blank-holder force (2.7, 7.5, 13, 16.5) kN
- (2) Temperature (30, 70, 110, 150) °C
- (3) Blank diameter (110, 120) mm
- (4) Blank thickness (2, 3) mm

Design of experiments was performed based on Taguchi L16 orthogonal array as shown in Table 4. To evaluate the formability in experiments, the following quantities were used to assess the effects of process variables on the forming behavior of the FML:

- (1) Maximum drawing force,
- (2) Wrinkling (number of wrinkles \times height of wrinkles),
- (3) Delamination,
- (4) Failure by tearing or fracture.

The factor of maximum drawing force was measured from the punch force displacement curve and wrinkling is the product of number and height of wrinkles. Moreover, a qualitative study was performed on delamination and depth at failure as two other measures of the formability of the FML.

5. RESULTS AND DISCUSSION

5. 1. Effect of Process Variables The experiments were carried out to investigate the maximum drawing force and wrinkling in the specimens. The effect of each parameter on the maximum drawing force and number and height of wrinkles was investigated by using Minitab software. It has to be mentioned that only the wrinkles of the first order were investigated. The height of the wrinkle (H) is defined as shown in Figure 8. Results based on the variations of process variables are presented in Table 5. The formed laminates are shown in Figure 9. The effect of blank-holder force on the formability of the FML system is investigated for laminates formed at four blank-holder forces. As shown in Figure 10, the maximum drawing force (F_m) increases with increasing the blank-holder force. Increasing the blank-holder force rises the friction between the blank and die, and blank and blank-holder, and consequently, drawing force will tend to increase Figure 9 shows that the blank-holder force increases from left to right in each row which in turn causes decreasing of wrinkling.

Furthermore, the product of number and height of wrinkles decrease as the blank-holder force increases (see Figure 11).



Figure 7. The 60 ton hydraulic press and die set.

TABLE 4. Design of experiments based on Taguchi L16 orthogonal.

	Blank-holder force (kN)	Temperature (°C)	Diameter (mm)	Thickness (mm)
1	2.7	30	110	2
2	2.7	70	110	2
3	2.7	110	120	3
4	2.7	150	120	3
5	7.5	30	110	3
6	7.5	70	110	3
7	7.5	110	120	2
8	7.5	150	120	2
9	13.0	30	120	2
10	13.0	70	120	2
11	13.0	110	110	3
12	13.0	150	110	3
13	16.5	30	120	3
14	16.5	70	120	3
15	16.5	110	110	2
16	16.5	150	110	2

The temperatures of FMLs and die set were raised to the given levels before forming. When temperature increases, F_m decreases sharply; however, the wrinkling increases slightly. (see Figures 10 and 11). Easy forming of polypropylene in this range of temperature causes the first event. However, more wrinkling can be attributed to the extra flexibility of polypropylene when the temperature is near its melting point. Figure 9 shows that the temperature increases from down to top in each column which causes increasing of wrinkling. There were some tearing in the lowest row, samples 5, 9 and 13 which were due to their higher blank-holder forces and lower temperatures compared to other samples.

In addition to independent effects of temperature and blank-holder force, the interaction effects between these two parameters affect the wrinkling of the laminates. It cannot be expected to remove the wrinkling at the low blank-holder force, however, for the high blank-holder force the wrinkling can be removed if the temperature sufficiently increases to prevent tear of the laminates.

Observation of formed laminates indicated the effect of diameter and thickness of blank on drawing force; for instance the maximum drawing force (F_m) increases as the blank diameter changes from 110 mm to 120 mm and thickness from 2 mm to 3 mm (Figures 10 and 11). Increasing the blank diameter causes rising of friction force, and therefore, F_m increases. Moreover, the variation of stress across the thickness of the blank shows an increase in stress from the middle surface to the outer surface of the blank. Therefore, by increasing the thickness of blank, the amount of maximum stress rises and the drawing force increases. The wrinkling increases slightly as the blank diameter becomes larger. Furthermore, it decreases when the thickness increases.

5. 2. Load-displacement Curve Load-displacement curve is one of the most important parameters to study in deep drawing processes. It indicates several features of the process, including required force, depth of drawing and the onset of failure by tearing or fracture. Failure and delamination are two important phenomena that occur in deep drawing of laminated materials.

The depth at which the failure occurred during the forming process was used as a measure of the formability of a sheet. Laminates that exhibited major failure by tearing or fracture were detectable in the punch force–displacement curve. When tearing or fracture occurs during forming, energy is released which can lead to a sharp drop in the punch force–displacement curve. (see Figure 12 for samples 13 and 14). A failure has occurred for the sample 13 which is clear from the difference of the two curves. Figure 13 shows the experimental and numerical results for load-displacement curves of formed specimen of the sample 1 at 30° C. The comparison between the results shows that the experimental curve follows the same trend

predicted by simulations of draw force in a good accuracy. Moreover, the location of wrinkles predicted by FE method is also in a good agreement with the experimental results. A small difference between the shapes of wrinkles in actual specimen and modeling was observed. This difference can be explained by the conditions of applied blank-holder force, i.e. in FE modeling force directly applied to reference point of blank-holder, while in actual test eight springs were used.

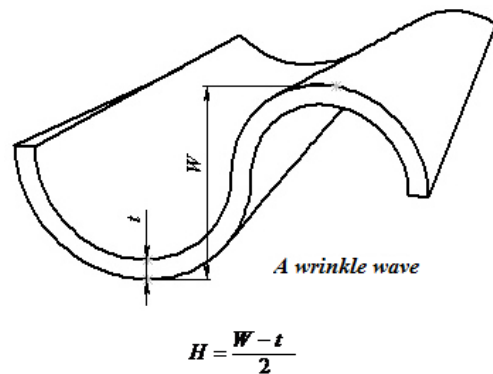


Figure 8. Measuring wrinkle height (H) in experiments.

TABLE 5. Maximum drawing force and number and height of wrinkles of test specimens

	Maximum drawing force (kN)	Number of wrinkles	Height of wrinkles(mm)
1	40.69	24	1.1875
2	24.46	31	0.7125
3	32.19	28	0.6625
4	26.78	25	0.7750
5	44.32	2	0.0000
6	33.88	12	0.2875
7	27.58	22	0.6250
8	23.30	26	0.5750
9	44.40	12	0.7875
10	36.68	10	0.6375
11	29.13	19	0.1500
12	24.12	26	0.2875
13	49.03	0	0.0000
14	41.78	24	0.3125
15	21.80	26	0.3750
16	20.25	30	0.0750



Figure 9. Runs of FML samples based on table of design of experiments.

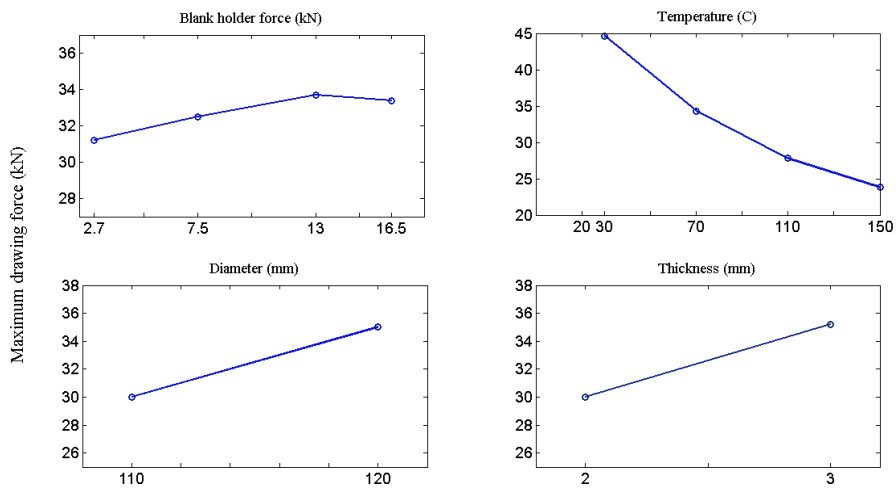


Figure 10. Maximum drawing force versus process variables.

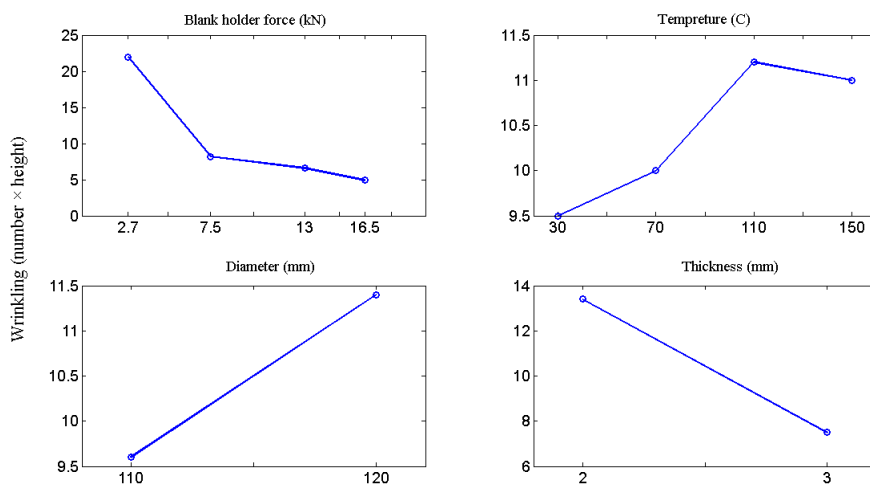


Figure 11. Wrinkling versus process variables.

6. CONCLUSIONS

The industrial applications of FML systems show clearly that various aspects of these materials, especially their forming processes are highly required to be investigated. In the current study, the deep drawing of thermoplastic based FML using aluminum as metal and glass-fiber reinforced polypropylene as composite was investigated and the forming behavior was studied. The experimental results indicate that the general effect of blank-holder force on the failure mode in FMLs is similar to custom metals and it limits the draw depth by the onset of wrinkling or fracture. Moreover, the effects

of blank diameter and blank thickness of the FML in deep drawing are also similar to custom metals. There were some tearing in samples 5, 9 and 13 which were because of higher blank-holder forces and their lower temperatures compared to the other samples. It demonstrates that a high interaction between the temperature and the blank-holder force is required to remove the wrinkling. The simulations showed that the draw force for this process may be predicted with a good accuracy; however, due to the multi-layers and non-isotropic nature of the FMLs, the FE simulation of this material is very complicated.

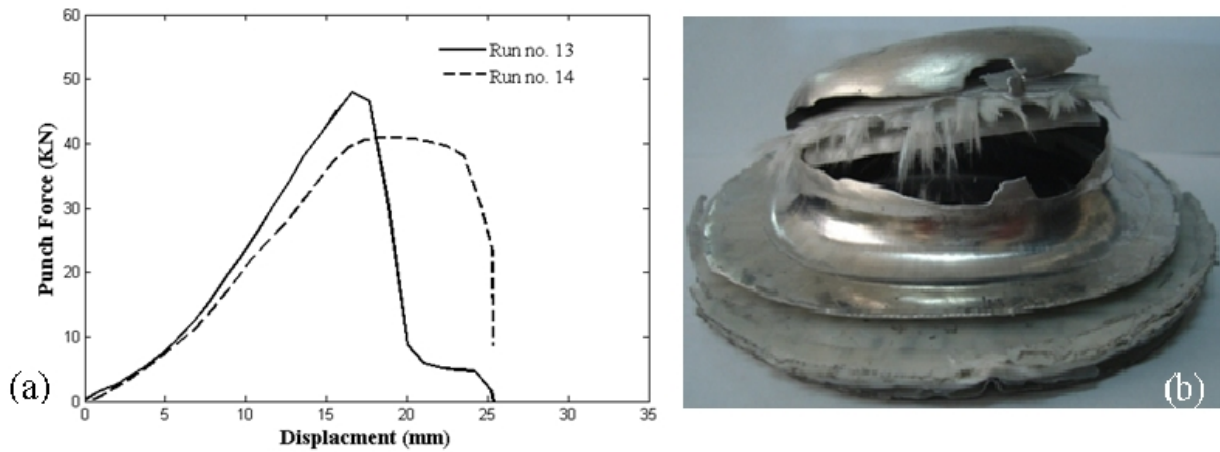


Figure 12. (a) Comparison between force-displacement curves of runs No. 13 and 14, (b) failure and delamination in run No. 13.

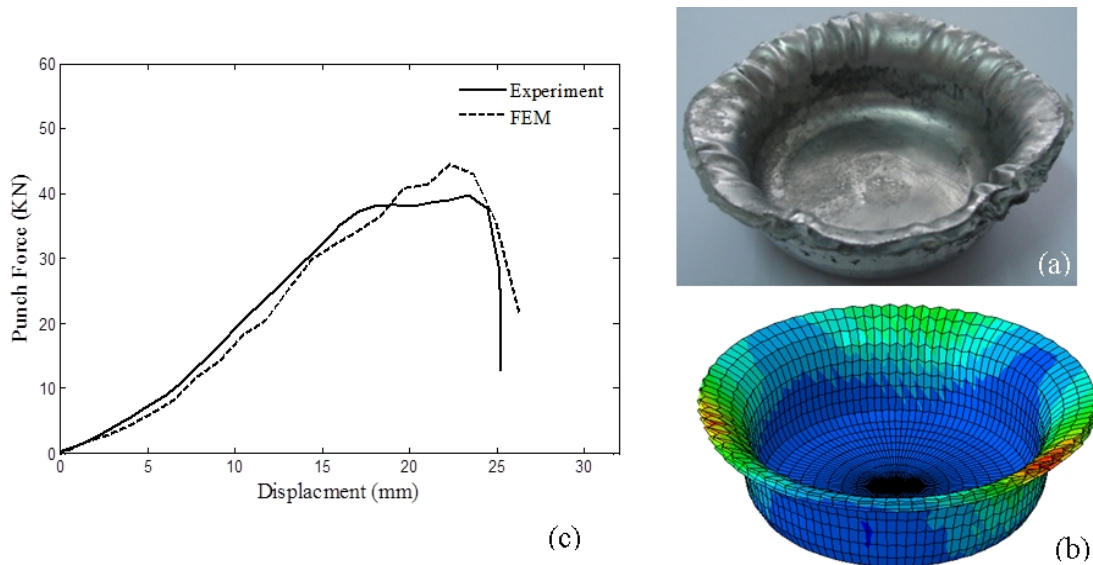


Figure 13. (a) Experimentally and (b) numerically formed sandwich sheet of sample No. 1, (c) comparison between the experimental and numerical load-displacement curves.

7. REFERENCES

1. Wang, L., Chan, L.C. and Lee, T.C., "Process modeling of controlled forming with variant blank holder force using RSM method", *International Journal of Machine Tools and Manufacture*, Vol. 47, (2007), 1929-1940.
2. Padmanabhan, R., Oliveira, M.C., Alves, J.L. and Menezes L.F., "Influence of process parameters on the deep drawing of stainless steel", *Finite Elements in Analysis and Design*, Vol. 43, (2007), 1062-1067.
3. Özek, C. and Ünal, E., "Optimization and Modeling of Angular Deep Drawing Process for Square Cups", *Materials and Manufacturing Processes*, Vol. 26, (2011), 1117-1125.
4. Arab, N. and Nazaryan, E., "Analytical modeling of axisymmetric sheet metal forming", *International Journal of Engineering*, Vol. 24, (2011), 55-63.
5. Rezaiee-Pajand, M. and Moayyedean, F., "A closed-form non-linear solution for plastic flange wrinkling of circular plates in deep drawig process", *International Journal of Engineering*, Vol. 23, (2010), 203-214.
6. De Magalhães Correia, J.P. and Ferron, G., "Wrinkling of anisotropic metal sheets under deep-drawing: analytical and numerical study", *Journal of Materials Processing Technology*, Vol. 155-156, (2004), 1604-1610.
7. Mosse, L., Cantwell, W., Cardew-Hall, M., Compston, P. and Kalyanasundaram, S., "Effect of process temperature and blank-holder force on the forming of fibre metal laminate systems", Proceedings of 11th European conference on composite materials, Rhodes, Greece, 2004.
8. Mosse, L., Cantwell, W., Cardew-Hall, M., Compston, P. and Kalyanasundaram, S., "Investigation of process temperature on the cup forming of fibre-metal-laminate systems", *International Conference on Sheet Metal*, (2005).
9. Gresham, J., Cantwell, W., Cardew-Hall, M. J., Compston, P. and Kalyanasundaram, S., "Drawing behaviour of metal-composite sandwich structures", *Composite Structures*, Vol. 75, (2006), 305-312.
10. Morovvati, M.R., Mollaei-Dariani, B. and Asadian-Ardakani, M.H., "A theoretical, numerical, and experimental investigation of plastic wrinkling of circular two-layer sheet metal in the deep drawing", *Journal of Materials Processing Technology*, Vol. 210, (2010), 1738-1747.
11. Atrian, A. and Fereshteh-Saniee, F., "Deep drawing process of steel/brass laminated sheets", *Composites Part B: Engineering*, Vol. 47, (2013), 75-81.
12. Davey, S., Das, R., Cantwell, W. and Kalyanasundaram, S., "Forming studies of carbon fibre composite sheets in dome forming processes", *Composite Structures*, Vol. 97, (2013), 310-316.
13. American Society for Testing Materials, "Annual book of ASTM standards", ASTM International, (2005).
14. Caprino, G., Iaccarino, P. and Lamboglia, A., "The effect of shear on the rigidity in three-point bending of unidirectional CFRP laminates made of T800H/3900-2", *Composite Structures*, Vol. 88, (2009), 360-366.
15. Kaneko, T., "On Timoshenko's correction for shear in vibrating beams", *Journal of Physics D: Applied Physics*, Vol. 8, (1975), 1927-1936.
16. Kennedy, Graeme J., Hansen, Jorn S., Martins, Joaquim R. R. A., "A Timoshenko beam theory with pressure corrections for layered orthotropic beams", *International Journal of Solids and Structures*, Vol. 48, (2011), 2373-2382.
17. Timoshenko, S. P., "On the transverse vibrations of bars of uniform cross section", *Philosophical Magazine*, Vol. 43, (1922), 125-131.
18. ABAQUS Inc, "ABAQUS analysis: user's manual", (2006).
19. Parsa, M.H. and Ettehad, M., "Prediction of delamination during deep-drawing of Steel-polymer-steel sandwich sheet materials", *International Conference on Technology of Plasticity*, (2008), 980-985.

An Investigation into the Deep Drawing of Fiber-metal Laminates based on Glass Fiber Reinforced Polypropylene

A. Rajabi, M. Kadkhodayan

Department of Mechanical Engineering, Ferdowsi University of Mashhad, Mashhad

چکیده

PAPER INFO

Paper history:

Received 27 June 2013

Received in revised form 28 August 2013

Accepted 14 September 2013

Keywords:

Deep Drawing

Fiber-metal Laminate

Design of Experiments

Finite Element Analysis

چند لایه‌های فلز-کامپوزیت نوع جدیدی از مواد کامپوزیتی هستند که می‌توانند معایب کامپوزیت‌های مرسوم را از لحاظ نرمی، شکل پذیری، ضربه پذیری و حاشیه خرابی بهبود بخشند. رفتار کششی یک چند لایه فلز کامپوزیتی گرم‌انرم شامل هسته چند لایه کامپوزیتی با پایه پلی‌پروپیلن تقویت شده با الیاف شیشه و لایه بیرونی آلومینیوم 1200-O بررسی شده است. تاثیر متغیرهای فرایند شامل نیروی ورق‌گیر، دما، قطر و ضخامت نمونه روی رفتار کششی فلز-کامپوزیت مطالعه شده است. برای کاهش تعداد آزمایش‌ها و بررسی متغیرهای فرایند روی ماکزیمم نیروی شکل دهی و چروکیدگی نمونه‌ها، از طراحی آزمایش‌ها استفاده شده است. نتایج آزمایش‌ها نشان دادند که تاثیر کلی نیروی ورق‌گیر روی واماندگی فلز-کامپوزیت و اثر قطر نمونه و ضخامت نمونه یک فلز-کامپوزیت در کشش عمیق مشابه تاثیر این متغیرها بر روی فلزات رایج می‌باشد. علاوه بر آن، نتایج نشان دادند که برای حذف چروکیدگی، اثر همزمان دما و نیروی ورق‌گیر به میزان بالایی مورد نیاز است. ثابت‌های مهندسی کامپوزیت با پایه پلی‌پروپیلن تقویت شده با الیاف شیشه با استفاده از تئوری تیر تیموشنکو به دست آمدند. شبیه سازی عددی با نرم افزار اجزاء محدود آباکوس انجام و مطابقت مناسبی بین نتایج تجربی و شبیه سازی مشاهده شد.

doi: 10.5829/idosi.ije.2014.27.03c.01